Geophys. J. Int. (2003) **155,** 367–378

Revisiting the Jurassic geomagnetic reversal recorded in the Lesotho Basalt (Southern Africa)

Michel Prévot,[1] Neil Roberts,[2] John Thompson,* Liliane Faynot,[1] Mireille Perrin[1] and Pierre Camps[1]

[1] *Laboratoire de Tectonophysique, CNRS-UM2, Université de Montpellier II,* 34095 *Montpellier Cedex* 5, *France. E-mail: Michel.Prevot@dstu.univ-montp2.fr.*
[2] *Magnetic Resonance and Image Analysis Research Centre (MARIARC), University of Liverpool,* PO Box 147, *Liverpool* L69 3BX*, UK*

Accepted 2003 April 9. Received 2003 April 9; in original form 2003 January 20

SUMMARY

We carried out a detailed and continuous palaeomagnetic sampling of the reversed to normal geomagnetic transition recorded by some 60 consecutive flow units near the base of the Lesotho Basalt (183 ± 1 Ma). After alternating field or thermal cleaning the directions of remanence are generally well clustered within flow units. In contrast, the thermal instability of the samples did not allow us to obtain reliable palaeointensity determinations. The geomagnetic transition is incompletely recorded due to a gap in volcanic activity attested to both by eolian deposits and a large angular distance between the field directions of the flows underlying or overlying these deposits. The transition path is noticeably different from that reported in a pioneering work carried out in 1962. The most transitional virtual geomagnetic poles (VGPs) are observed after the volcanic hiatus. Once continents are replaced in their relative position 180 Myr, the post-hiatus VGPs cluster over Russia. However, two successive rebounds from that cluster are found, with VGPs reaching repeatedly the Eastern Asia coast. Thus, the VGP path is not narrowly constrained in palaeolongitude. The decrease in intensity of magnetization as the field deviates from the normal or reversed direction suggests that the decrease in field magnitude during the reversal reached 80–90 per cent. We conclude that although the reversal is of a dipole of much weaker moment than that which existed on average during Cenozoic time, the characteristics of the reversing geodynamo seem to be basically similar.

Key words: field reversal, geomagnetism, Jurassic, palaeomagnetism, palaeointensity, Southern Africa.

1 INTRODUCTION

Brynjolfsson (1957) and Sigurgeirsson (1957) were probably the first workers to report the occurrence of lava flows with intermediate directions of remanence between two volcanic magnetozones of opposite polarity. They suggested that these intermediate directions, observed on Icelandic lava flows of Upper Cenozoic age, offer a record of the transitional state of the geomagnetic field when changing from one polarity state to the other. A few years later, from an extensive magnetic study of some 150 cores recovered along a 1300 m thick section of the Early Jurassic Lesotho Basalt (southern Africa), van Zijl *et al.* (1962a,b) reported an impressive line of observations in favour of a geomagnetic origin of the progressive reversal of remanence in successive lava flows, as opposed to the self-reversal mechanism proposed by Néel (1951, 1952). In the Maseru area, these authors were able to describe a transition zone extending between 290 and 442 m above the base of the lava sequence (Fig. 1) between underlying reversed flows and the overlying normal ones. The most important observations of van Zijl *et al.* (1962a) in favour of the genuine character of field reversal were as follows: (1) baked sediments exhibit the same remanence direction as the overlying flow; (2) reversed lava flows cut by normally magnetized dykes become normally magnetized as one approaches the contact; and (3) lava flows and sediments also acquire a thermoremanent magnetization (TRM) parallel to the laboratory field direction whatever their natural remanent magnetization (NRM) polarity. Moreover, in their second paper van Zijl *et al.* (1962b) were the first workers to try to determine the palaeostrength of the geomagnetic field while reversing. Comparing the intensity of a total TRM acquired in the laboratory with that of NRM (both partially demagnetized by an alternating field, AF), they concluded that the field intensity decreased by a factor of about 4–5 during the reversal. This total TRM palaeointensity method is no longer in use because it offers no possibility to detect the changes in TRM capacity occurring during laboratory heating at high temperature (650 °C in van Zijl *et al.*'s 1962b experiments).

The present study was undertaken with the aim of obtaining a more precise description of the Lesotho geomagnetic reversal. In

*Formerly at: Laboratoire de Géomagnétisme, CNRS and Université de Paris 6, 94107 Saint-Maur Cedex, France. Now at: 8 rue Taylor, 75010 Paris, France.

© 2003 RAS

Downloaded from https://academic.oup.com/gji/article/155/2/367/596587 by Univ of California, San Diego Library - INACTIVE user on 11 March 2025

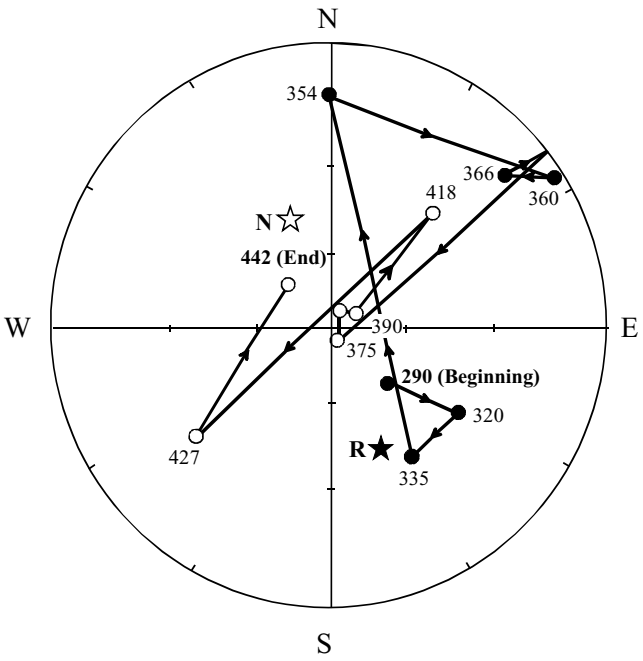

Figure 1. Stereographic projection of the cleaned direction of remanence of successive flows from the Lesotho transition zone in Maseru area according to van Zijl *et al.* (1962a) (redrawn). The figures by the dots indicate the approximate flow elevation in metres above the base of the lava sequence.

the original study, not all the consecutive flows were sampled and only one (long) core was collected from each sampled flow. Apparently, this field reversal occurred during a period of long-term dipole low (Prévot *et al.* 1990; Perrin & Shcherbakov 1997). According to Kosterov *et al.* (1997) the average field intensity during the Early Jurassic was only half of the Late Cenozoic value. While there are several well-documented records of Upper Cenozoic reversals (Mankinen *et al.* 1985; Prévot *et al.* 1985a,b; Chauvin *et al.* 1990; Kristjansson & Sigurgeirsson 1993; Goguitchaichvili *et al.* 1999; Leonhardt *et al.* 2002), the Lesotho reversal is to date the only detailed volcanic record of a geomagnetic transition that occurred during a long period of dipole low. This gives a particular interest to this reversal, since it is not yet known whether the characteristics of geomagnetic reversal depend upon the magnetic moment of the dipole field that existed during the preceding and following epochs of stable polarity.

2 SAMPLING AND LABORATORY PROCEDURES

Geology and sampling

The Lesotho Basalt (Fig. 2) is part of the widespread volcanism that occurred in Southern Africa in Lower Jurassic times. Two sections were studied by van Zijl *et al.* (1962a,b): Bushmen's Pass (near Maseru) and Sani Pass. Because the latter section is more weathered, we focused our efforts on the Bushmen's Pass section. In the course of a generalized sampling of the reverse zone, a few flows were also collected near Rhodes, some 150 km south of Bushmen's Pass. Four of these flows were found to be transitional and the relevant data will be presented here.

In the Maseru area, four sections (from bottom to top: Y, Z, X and R) were sampled along or in the vicinity of the road going up from Nazareth to Bushmen's Pass (Fig. 3). These sections stratigraphically overlap with each other. Unambiguous correlations from one section to the other could be made between flows or groups of flows using stratigraphic evidence and directions of remanence. Altogether, we think that our sampling was continuous between 2010 m (base of Y) and 2350 m (top of R). The successive flows were numbered upwards (Y7–Y21; Z1–Z10; X1–X25; R1–R12). A total of 56 distinct flows (785 cores) were sampled (four to eight cores per flow). The four transitional flows from the Rhodes area were collected at two sites within the bed of Bell river (latitude 30° 45′ 37″ S and longitude 28° 02′ 47″ E for RH4 and RH5; latitude 30° 45′ 49″ S and longitude 28° 03′ 22″ E for RH7 and RH8, collected near Naude's Neck monument).

Along the Bushmen's Pass composite section, the average flow thickness is approximately 6 m. Individual values vary from 1 to 20 m. Typically, the flow base is characterized by vertically elongated vesicles, which differ markedly from the more spherical or horizontally flattened vesicles from the upper parts of flows. Ropy flow tops were occasionally observed. A major feature of the Lesotho Basalt sequence is the occurrence of a thin sedimentary level within the geomagnetic transition zone (van Zijl *et al.* 1962a). Along the Busmen's Pass sequence, the horizon of a sedimentary lens, each up to 1.5 m thick and several metres long, was observed near elevation 2160 m. We were able to trace this discontinuous sedimentary layer over 1 km along the Western slope of the Thaba-Tseka mountain (Fig. 3). We will see below that this horizon corresponds to a distinctive break in the geomagnetic record. There is no evidence for a regional tilting of the lava pile (Hargraves *et al.* 1997).

Fitch & Miller (1971, 1984) reported the first K-Ar and $^{39}Ar/^{40}Ar$ values for the Lesotho Basalt at Bushmen's Pass. They concluded that this lava section erupted very rapidly at some time close to 193 Ma. More recent $^{39}Ar/^{40}Ar$ dating (Duncan *et al.* 1997), once recalculated using the standard hornblende monitor Mmhb-1 (523.4 Ma, astronomically tuned), provides a mean age of 183 ± 1 Ma for the Lesotho formation as a whole. Palaeomagnetic data are compatible with an extremely rapid eruption of the total 1400 m thick sequence. Considering that the reversal is recorded over a thickness of some 150 m and that the mean duration for field reversal is of the order of 5000–6000 yr (Kristjansson 1985), the eruption of the Lesotho Basalt might have lasted for some 50 000 yr or so. Thus, the mean age of the lava pile is also the best radiometric estimate of the age of the reversal, which has therefore to be considered as Toarcien. According to the geomagnetic reversal timescale of Gradstein *et al.* (1994), the Lesotho reversal might be either 182.4 or 183.2 Myr old.

Laboratory procedures

We first determined the 2 week viscosity index (Thellier & Thellier 1944; Prévot 1981) of one specimen from each core, with the exception of cores from X-section, which were first magnetically analysed at the Liverpool laboratory. Then another specimen from each core was progressively demagnetized by alternating fields. Several specimens from each flow were also demagnetized by stepwise heating in zero field in air. For each specimen, the direction of the characteristic remanent magnetization (ChRM) was calculated using principal-component analysis (Kirschvink 1980). A few flows were subjected to palaeointensity experiments using the Thellier original method (Thellier & Thellier 1959) and a high-vacuum furnace. Unfortunately, due to the poor magnetic stability of most of the Lesotho lava flows during heating (Kosterov & Prévot 1998),

Downloaded from https://academic.oup.com/gji/article/155/2/367/596587 by Univ of California, San Diego Library - INACTIVE user on 11 March 2025

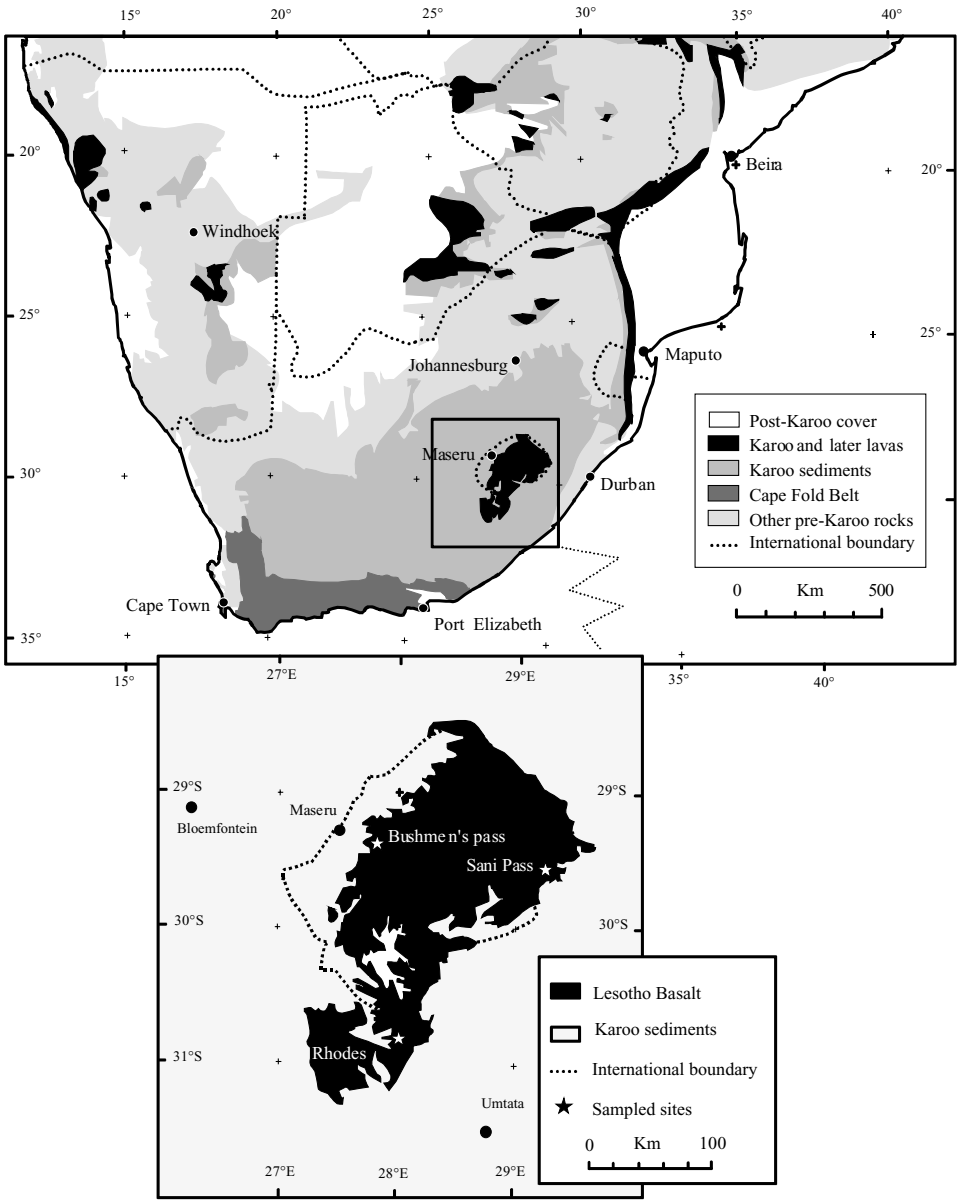

Figure 2. The three main sampling localities of the Lesotho reversal. Maps redrawn from Kosterov & Perrin (1996).

no really reliable palaeointensity data could be obtained. However, NRM(T) directions calculated from these experiments were used as a substitute to data from standard thermal cleaning to provide the ChRM direction of the specimens studied for palaeointensity purpose. This substitution is justified by the absence of noticeable CRM acquisition during palaeointensity experiments (Kosterov & Prévot 1998).

3 PALAEOMAGNETIC CHARACTERISTICS OF SAMPLES

As previously observed (Prévot 1981), the magnetic viscosity index v does not show a normal distribution (Fig. 4a) but rather a lognormal one (Fig. 4b). The mode on this figure corresponds to $v = 5$ per cent. Considering the age of the rocks, this is a rather weak value, in fact close to the average viscosity index found for subaerial lava flows of Upper Cenozoic age (Prévot 1981).

Examples of the orthogonal plots obtained from either AF or thermal progressive demagnetization are given in Fig. 5. As a general rule, a quite simple magnetic behaviour is observed in the lowermost (reversed) and the uppermost (normal) lava flows (Fig. 5a). With the exception of a small VRM, a single component is observed. Thermal and AF demagnetization yield the same direction of ChRM, although some deflection of the direction can sometimes be seen on the AF diagrams when approaching a completely demagnetized state.

For the median part of the composite section, the behaviour of the samples is not always as straightforward. As shown by Fig. 5(b), thermal cleaning appears more suitable than AF cleaning, even when the secondary component is small. It can be inferred from Fig. 5(c) that most of the difficulties encountered during AF cleaning are due to the acquisition of some parasitic magnetization as an anhysteretic remanent magnetization (ARM) or a rotational remanent magnetization (RRM), which progressively deflects the direction of remanence. In such specimens, thermal cleaning is necessary to reach an

Downloaded from https://academic.oup.com/gji/article/155/2/367/596587 by Univ of California, San Diego Library - INACTIVE user on 11 March 2025

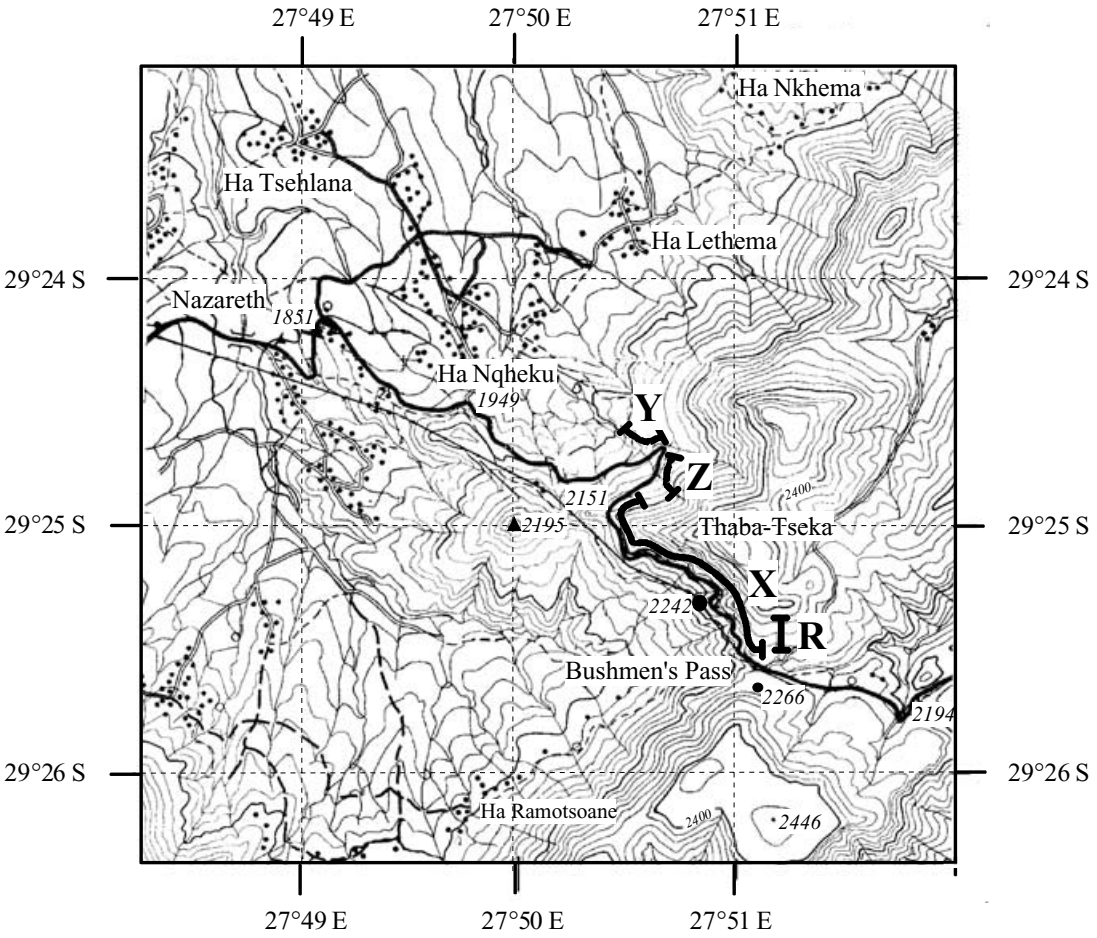

Figure 3. Precise location of the four sections sampled by us between Nazareth and Bushmen's Pass (Maseru area).

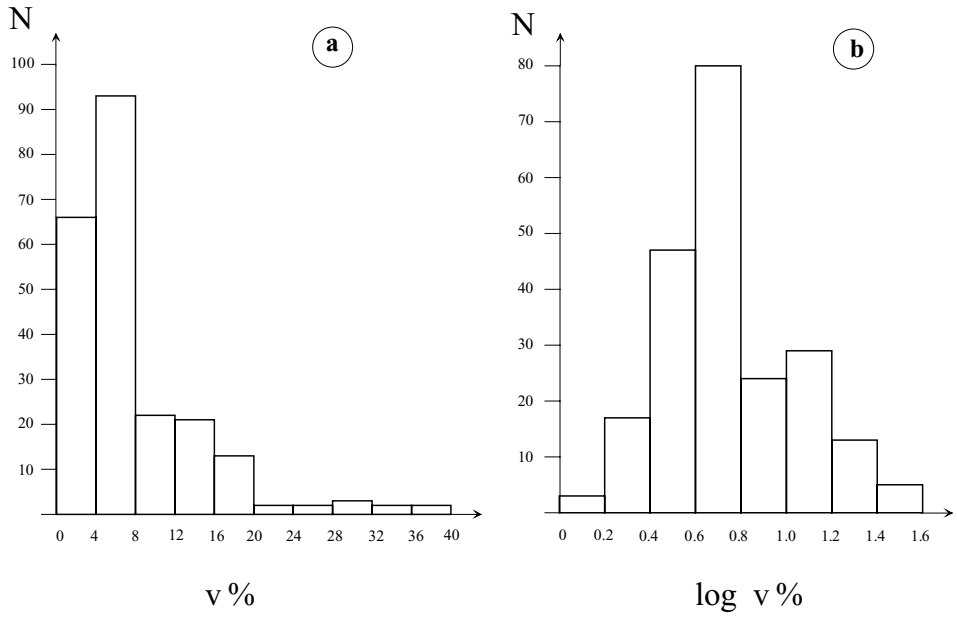

Figure 4. Distribution of magnetic viscosity index (see text) from a total of 224 specimens.

approximately zero-magnetization state in the specimen (Fig. 5c, specimen 86P133A).

Typically, the natural secondary components remain small in the flows from the transition zone and thermal treatment allows a precise determination of ChRM direction (Fig. 5d, specimen 86P482B). However, a few samples carry quite a large low-temperature secondary component, possibly of viscous origin for the example shown in Fig. 5(d) (specimen 86P128A). In a restricted

Downloaded from https://academic.oup.com/gji/article/155/2/367/596587 by Univ of California, San Diego Library - INACTIVE user on 11 March 2025

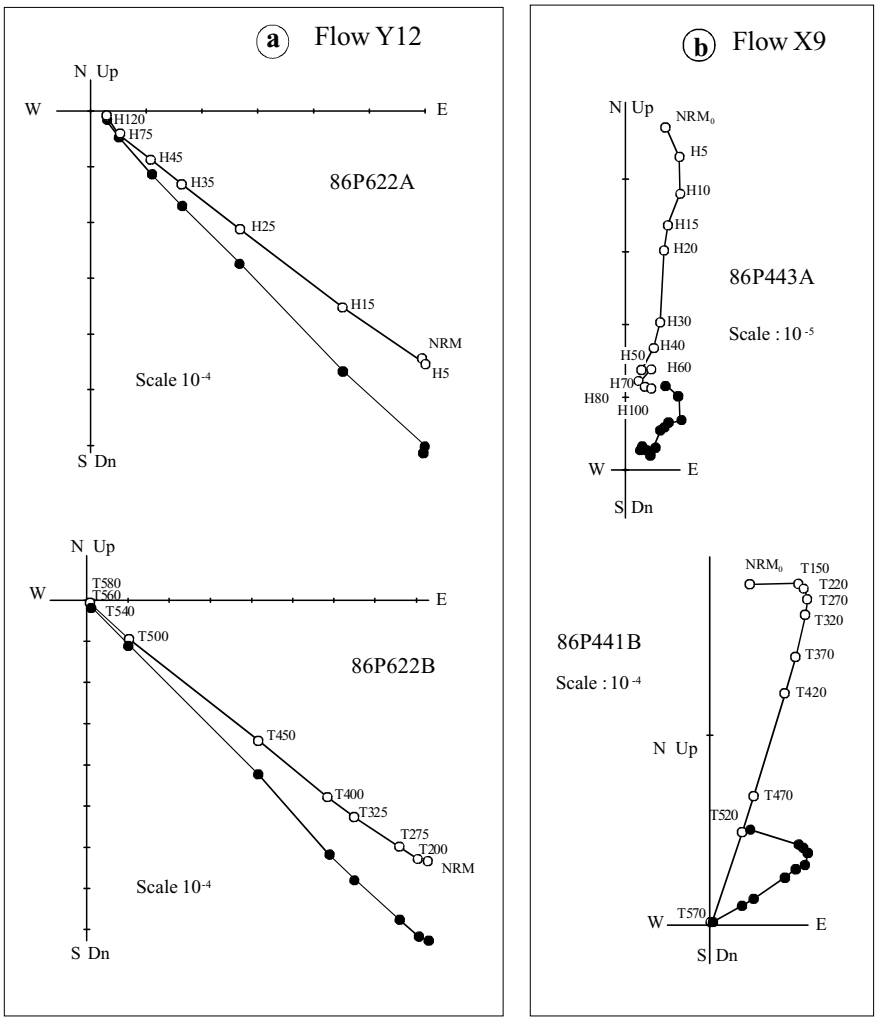

Figure 5. (a–d) Examples of orthogonal thermal or alternating field demagnetization diagrams (stratigraphic coordinates) for a total of eight specimens from one flow from the reversed zone (Y12) and three flows from the transition zone (lower part, Z10; middle part, X9; upper part, X15). Full (empty) circles represent data projected on to the (one) horizontal (vertical) plane. Scale bars correspond to specific magnetization (A m^2 kg^{-1}). Cleaning steps are labelled as either T (temperature in °C) or H (peak field in mT).

area around Bushmen's Pass, corresponding to the uppermost flows of the X-section (above X22), several cores were found to carry a large IRM (in spite of the precautions taken in the field to avoid sites struck by lighting), which made it impossible to determine ChRM directions.

The flow average direction was in general calculated from the combination of the remanence directions of both thermally and AF cleaned specimens. Although the cleaning range used for principal-component analysis was variable from specimen to specimen, the ranges 400–550 °C or 20–50 mT are rather typical. The flow directions thus obtained are listed in Table 1. The quality of the data is very good both in the reversed and normal zones (almost 95 per cent of sampling sites with dispersion parameter $k > 100$), but only fairly good in the transition zone (70 per cent of sampling sites with dispersion parameter $k > 100$).

4 DESCRIPTION OF THE COMPOSITE GEOMAGNETIC TRANSITION RECORD

Stratigraphic observations and palaeomagnetic data both agree that the four sections Y, Z, X and Z overlap slightly, which allows reconstruction without any gap of the palaeomagnetic behaviour recorded by the Bushmen's Pass sequence. The composite record consists of 36 'distinct' palaeomagnetic directions (Table 2 and Fig. 6) distinguished from each other using the method of Mankinen *et al.* (1985). Each of these directions defines a 'palaeomagnetic unit'. One-third of these palaeomagnetic units are defined from several (up to six) consecutive lava flows, yielding the same direction (overlapping α_{95} semi-angles) called 'directional flow groups' by Mankinen *et al.* (1985). The limits of the transition zone were defined from the reversal angle (Prévot *et al.* 1985b) of each palaeomagnetic unit. The reversal angle of a palaeomagnetic unit is the angular distance between the palaeomagnetic direction of this unit and the direction of either the normal or reversed mean field, whichever is closer. The beginning (end) of the transition zone was chosen as corresponding to the first (last) flow from a sequence of at least two consecutive palaeomagnetic units with reversal angle lying outside the θ_{95} semi-angle of individual directions. Following the results of the palaeosecular variation study of the normal and reversed magnetozones of the Lesotho Basalt carried out by Kosterov & Perrin (1996), θ_{95} was taken to be equal to 24°.

Downloaded from https://academic.oup.com/gji/article/155/2/367/596587 by Univ of California, San Diego Library - INACTIVE user on 11 March 2025

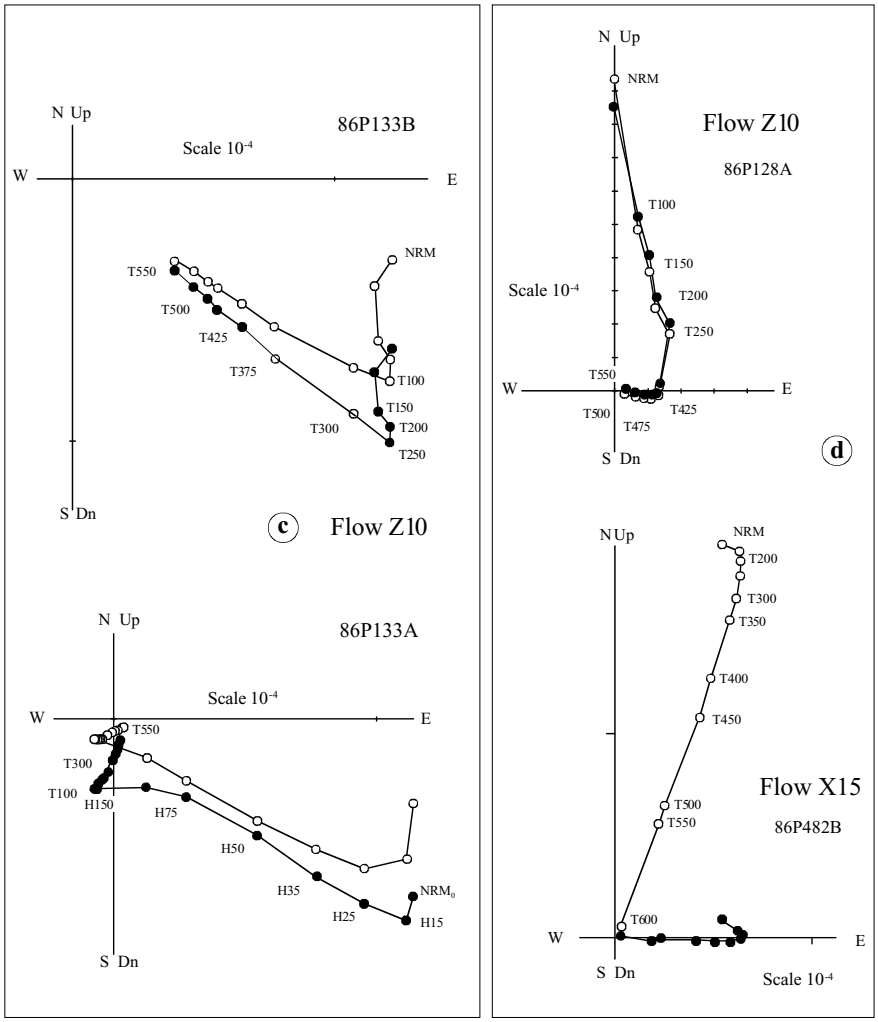

Figure 5. (*Continued*.)

The transition path is obviously discontinuous. A large angular gap is observed at the level of the sedimentary lens (elevation 2155 m) between directions 11 and 12. This gap was first observed by van Zijl *et al.* (1962b), who also found it along the Sani Pass section, some 130 km east of Bushmen's Pass. The sedimentary lenses display cross-stratification of eolian origin. Obviously, the palaeomagnetic gap is due to a pause in volcanic activity. None of the transitional directions deviates by more than 54° from the steady field direction (Table 2), which suggests that the volcanic pause was coincident with the most transitional field configurations. The directional path presently obtained (Fig. 6) is more detailed and presents obvious differences from that reported by van Zijl *et al.* (1962b). These differences probably result from the fact that this pioneering study was based on a discontinuous sampling of the flow sequence, with generally only a single core from each sampled flow, and a moderate AF cleaning, sometimes insufficient to erase VRM or IRM due to lightning. Moreover, as we showed above, AF treatment of some samples can yield misleading results. The zigzag behaviour of the transitional field directions described by these workers (Fig. 1) is not confirmed by our data. Instead, our record is compatible with rather gradual changes in direction during the two parts (pre- and post-gap) of the reversal. Furthermore, a rather complex pattern is observed during the final stages of the transition.

The virtual geomagnetic poles (VGP) positions (Table 2) were first calculated as usual with Africa in its present position, and then with Africa rotated back to its 180 Myr old position according to Morgan (1983). This palaeoreconstruction assumes fixity of the Atlantic and Indian Ocean hotspot system as a whole. Fig. 7 represents the palaeo-VGP path of the Lesotho reversal on to the 180 Myr old plate reconstruction proposed by Morgan (1983). The geographic palaeopole used for that figure is the global palaeomagnetic pole for the period 175–200 Ma as calculated by Prévot *et al.* (2000) from a selected data set of palaeomagnetic data from all continents obtained from magmatic rocks. Most of the transitional VGPs plot over Russia. However, two successive 'rebounds' (Watkins 1969) are observed with extreme VGP positions close to the margin of the Eurasia and Pacific plates.

In the absence of direct palaeointensity determinations, we tried to obtain a qualitative description of field palaeostrength changes during this transition using cleaned remanence intensities as a proxy. This approach was already used by several authors (Dagley & Wilson 1971; Kristjansson 1985; Chauvin *et al.* 1990; Camps & Prévot 1996). In the case of the Lesotho Basalt, the use of this indirect method seems reasonable considering the petrographic monotony of this volcanic suite (Cox 1988) and the relative weakness of secondary magnetizations as compared with ChRM in most of the rock samples. Moreover, rather than using NRM intensity,

Downloaded from https://academic.oup.com/gji/article/155/2/367/596587 by Univ of California, San Diego Library - INACTIVE user on 11 March 2025

Table 1. Average ChRM directions and VGP coordinates of successive flows from Bushmen's Pass (sections Y, Z, X and R) and Rhodes sections. Palaeomagnetic units (PU) are numbered from 1 to 36 (see text), elevation corresponds to flow base, N is the number of specimen directions used, I is inclination (degrees), D is declination (degrees), k is Fisher precision parameter, α_{95} is semi-angle of the 95 per cent confidence cone, PLA and PLO are the VGP latitude and longitude in degrees.

Flow label Bushmen's Pass (∼29.4°S, 27.8°E)	PU	Elevation (m)	N	I	D	k	α_{95}	PLA	PLO
Y7	1	2011	5	47.2	157.7	60	10	−70.5	115.4
Y8	2	2017	6	40.9	141.6	231	4.4	−55.2	118.5
Y9	2	2020	10	42.3	138.5	153	3.9	−52.9	115.3
Y10B	2	2021	7	42.1	136.0	389	3.1	−50.6	114.5
Y10A	2	2022	4	45.5	142.0	1033	2.9	−56.6	112.6
Y11	2	2023	5	42.7	138.4	598	3.1	−52.9	114.8
Y13	2	2033	8	41.3	140.0	372	2.9	−53.9	117.2
Y14	3	2040	9	47.5	131.9	118	4.8	−48.2	106.6
Y15	4	2046	5	50.6	121.5	899	2.6	−40.1	100.0
Y16	4	2052	9	49.4	120.3	202	3.6	−38.8	101.0
Y17	5	2060	6	55.2	129.0	2106	1.5	−47.0	95.6
Y18	5	2065	3	52.0	131.2	178	9.3	−48.4	100.5
Y19	5	2072	8	55.8	127.1	317	3.1	−45.6	94.4
Y20	6	2076	7	53.9	130.7	140	5.1	−48.3	97.7
Y21	6	2081	5	53.1	133.9	661	3.0	−50.8	99.4
Z1	6	2095	6	54.7	130.4	538	2.9	−48.1	96.5
Z2	7	2099	7	61.9	117.6	543	2.6	−39.1	84.2
Z3	7	2101	8	62.5	122.2	763	2.0	−42.4	83.6
Z4	8	2105	7	48.0	125.0	63	7.6	−42.5	103.9
Z5	9	2109	6	34.4	121.3	225	4.5	−36.0	114.9
Z6	10	2112	4	28.8	117.3	621	3.7	−31.0	116.9
Z7	11	2132	7	28.9	120.8	254	3.8	−34.1	118.5
Z9	11	2143	4	27.7	120.4	848	3.2	−33.4	119.1
Z10	11	2145	11	27.8	121.1	335	2.5	−34.1	119.4
X1	11	2145	3	28.6	122.8	338	6.7	−35.8	119.7
X2	11	2150	3	24.0	121.6	179	9.2	−33.5	122.0
X3	11	2154	5	28.2	122.8	353	4.1	−35.7	120.0
Sedimentary lens									
X4	12	2157	5	−23.8	5.5	75	8.9	72.3	45.7
X5	13	2160	5	−46.1	343.3	53	10.6	75.2	301.3
X6	14	2162	8	−5.6	9.3	81	6.2	62.0	47.9
X7	15	2180	3	−33.0	347.8	448	5.8	74.1	340.8
X8	16	2197	6	−15.6	356.5	275	4.0	68.3	18.4
X9	17	2200	5	−70.9	58.6	184	5.7	41.5	167.4
X10	18	2212	4	−73.6	50.0	376	4.7	45.0	174.5
X11	19	2218	3	−67.6	344.8	318	6.9	66.0	232.0
X12	20	2221	6	−77.1	64.5	101	6.7	37.0	179.7
X13	20	2226	7	−78.8	77.3	115	5.7	31.8	182.8
X14	21	2238	5	−71.5	91.9	73	9.0	23.1	170.6
X15	21	2245	6	−68.0	94.6	243	4.3	19.7	166.1
X16	22	2250	12	−63.7	43.1	171	3.3	52.8	155.2
X17	22	2254	8	−63.5	46.3	454	2.6	50.6	154.3
X18	22	2256	8	−61.4	51.4	284	3.3	47.1	150.0
X19	23	2260	8	−59.5	19.2	54	7.6	70.9	157.8
X20	24	2263	9	−31.2	356.7	76	5.9	77.1	13.5
X21	25	2266	6	−33.1	7.5	49	9.7	76.7	60.6
X23A	26	2281	5	−47.7	350.2	64	9.6	81.4	299.5
X23B	27	2287	3	−38.3	7.1	71	14.8	79.9	68.6
X24	27	2288	5	−30.2	7.0	30	14.0	75.3	55.3
X25	28	2292	5	−53.1	1.9	117	7.1	85.4	187.5
X26	29	2316	3	−14.4	4.7	16	31.8	67.5	40.0
R1	29	2296	3	−18.9	6.5	277	7.4	69.4	46.3
R2	29	2301	4	−020	5.3	146	7.6	70.2	43.3
R3	29	2306	4	−22.8	4.5	151	7.5	72.0	42.2
R4	29	2311	4	−19.8	0.6	212	6.3	70.8	29.6
R5	30	2316	5	−46.8	357.7	209	5.3	87.6	331.4
R6	31	2318	5	−54.3	0.9	708	2.9	84.5	200.0
R7	32	2321	5	−59.2	1.1	1363	2.1	79.4	203.2
R8	33	2325	5	−67.6	4.8	228	5.1	68.6	199.4

Downloaded from https://academic.oup.com/gji/article/155/2/367/596587 by Univ of California, San Diego Library - INACTIVE user on 11 March 2025

Table 1. (*Continued.*)

Flow label	PU	Elevation (m)	*N*	*I*	*D*	*k*	α_{95}	PLA	PLO
Bushmen's Pass (∼29.4°S, 27.8°E)									
R9	34	2330	5	−63.9	337.9	125	6.9	66.3	248.7
R10	35	2340	5	−66.7	351.6	1339	2.1	69.1	223.3
R11	36	2343	3	−65.9	335.0	428	6.0	63.2	246.4
R12	36	2350	4	−64.1	346.8	186	6.8	70.6	236.4
Rhodes (30.76°S. 28.05°E)									
RH4	14	1965	5	−5.6	4.3	225	5.1	61.7	37.2
RH5	14	1970	10	−8.8	6.3	220	3.3	63.0	42.0
RH7	around 22?	1975	5	−51.9	59.2	2673	1.5	40.3	136.5
RH8	around 22?	1980	6	−44.4	33.0	54	9.2	60.7	117.2

Table 2. Average ChRM directions and VGP coordinates (PLA, PLO) of consecutive palaeomagnetic units numbered from 1 (lowermost unit) to 36 (uppermost unit). Symbols are similar to those of Table 1 with in addition the reversal angle (Prévot *et al.* 1985b) in degrees, and the VGP palaeogeographic coordinates, palaeolatitude (PPLA) and palaeolongitude (PPLO), calculated from the position of the African plate 180 Myr according to Morgan (1983) and the global palaeopole position calculated by Prévot *et al.* (2000) for the period 175–200 Ma.

Palaeomag. Unit	Flow number(s)	*N*	*I*	*D*	*k*	α_{95}	δ	PLA	PLO	PPLA	PPLO
Reversed magnetozone											
1	Y7	5	47.2	157.7	60	9.9	6.2	−70.5	115.4	−59.3	160.9
2	Y8, Y9, Y10A, Y10B, Y11, Y13	41	42.3	139.2	273	1.4	17.0	−53.5	115.6	−46.9	141.3
3	Y14	9	47.5	131.9	118	4.8	17.8	−48.2	106.6	−45.8	130.2
4	Y15, Y16	14	49.8	120.7	289	2.3	23.5	−39.3	100.7	−40.7	118.6
5	Y17, Y18, Y19	17	54.9	128.5	375	1.8	17.5	−46.6	95.9	−48.7	120.1
6	Y20, Y21, Z1	18	53.9	131.5	276	2.1	15.9	−48.9	97.8	−49.8	123.8
7	Z2, Z3	15	62.2	120.0	607	1.6	21.9	−40.8	84.0	−48.7	104.4
8	Z4	7	48.0	125.0	63	7.6	21.7	−42.5	103.9	−42.1	123.6
Transitional magnetozone											
9	Z5	6	34.4	121.3	225	4.5	32.3	−36.0	114.9	−32.2	128.7
10	Z6	4	28.8	117.3	621	3.7	38.8	−31.0	116.9	−27.0	127.8
11	Z7, Z9, Z10, X1, X2, X3 Sedimentary lens	35	27.7	121.5	340	1.3	37.4	−34.4	119.7	−29.0	131.9
12	X4	5	−23.8	5.5	75	8.9	35.9	72.3	45.7	49.4	31.7
13	X5	5	−46.1	343.3	53	10.6	7.9	75.2	301.3	60.7	350.5
14	X6	8	−5.6	9.3	81	6.2	54.0	62.0	47.9	39.5	36.0
15	X7	3	−33.0	347.8	448	5.8	21.5	74.1	340.8	53.2	3.5
16	X8	6	−15.6	356.5	275	4.0	40.4	68.3	18.4	44.7	18.8
17	X9	5	−70.9	58.6	184	5.7	37.6	41.5	167.4	58.0	144.2
18	X10	4	−73.6	50.0	376	4.7	34.6	45.0	174.5	63.5	150.4
19	X11	3	−67.6	344.8	318	6.9	14.5	66.0	232.0	78.8	303.0
20	X12, X13	13	−78.1	71.0	113	3.9	38.7	34.2	181.4	55.2	167.8
21	X14, X15	11	−69.6	93.5	123	4.1	48.4	21.2	168.1	39.4	156.7
22	X16, X17, X18	28	−63.0	46.5	226	1.8	35.2	50.5	153.3	60.3	118.5
23	X19	8	−59.5	19.2	54	7.6	22.9	70.9	157.8	73.0	75.6
24	X20	9	−31.2	356.7	76	5.9	25.8	77.1	13.5	53.6	17.8
25	X21	6	−33.1	7.5	49	9.7	33.9	76.7	60.6	54.8	35.5
26	X23A	5	−47.7	350.2	64	9.6	9.4	81.4	299.5	64.1	1.8
27	X23B, X24	8	−33.3	7.0	39	9.0	28.5	77.1	59.0	55.0	34.6
28	X25	5	−53.1	1.9	117	7.1	13.9	85.4	187.5	70.7	25.7
29	X26, RI, R2, R3, R4	18	−19.2	4.3	70	3.9	35.6	70.1	40.3	46.9	29.7
Normal magnetozone											
30	R5	5	−46.8	357.7	209	5.3	16.8	87.6	331.4	64.8	17.3
31	R6	5	−54.3	0.9	708	2.9	13.2	84.5	200.0	71.8	23.0
32	R7	5	−59.2	1.1	1363	2.1	13.7	79.4	203.2	76.9	22.4
33	R8	5	−67.6	4.8	228	5.1	18.9	68.6	199.4	87.1	57.6
34	R9	5	−63.9	337.9	125	6.9	10.5	66.3	248.7	72.4	312.3
35	RI0	5	−66.7	351.6	1339	2.1	14.8	69.1	223.3	82.2	321.4
36	RII,RI2	7	−65.0	342.0	214	4.1	11.7	67.5	241.3	75.6	313.5

Downloaded from https://academic.oup.com/gji/article/155/2/367/596587 by Univ of California, San Diego Library - INACTIVE user on 11 March 2025

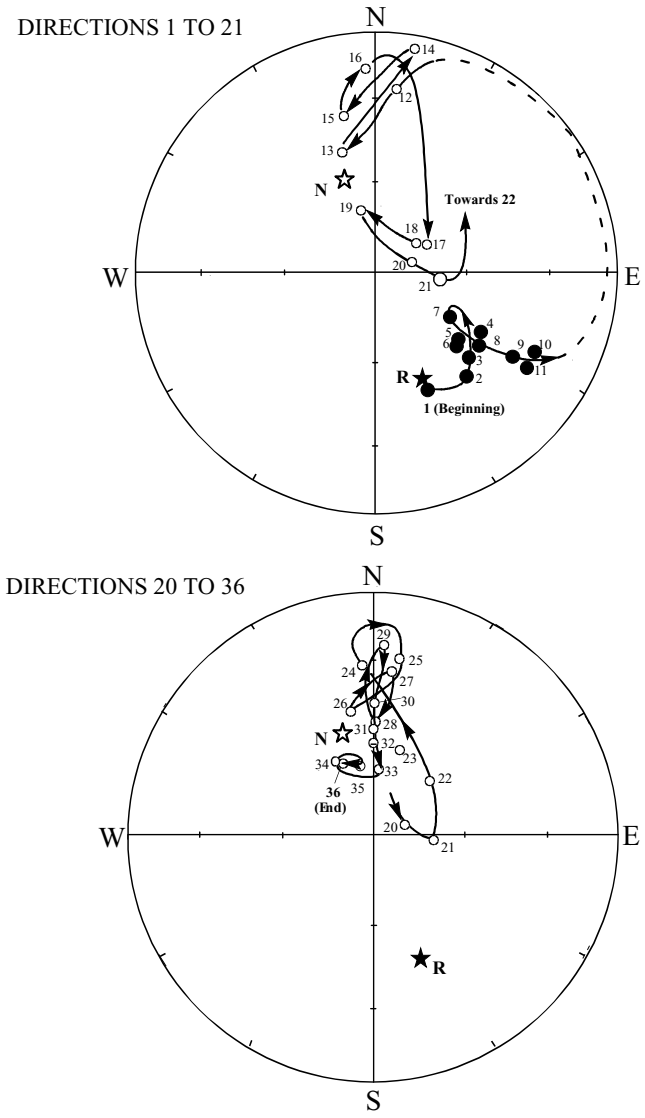

Figure 6. Equal-area projection of average ChRM directions of consecutive palaeomagnetic units (flow or group of consecutive flows) numbered from the reversed unit 1 (base of composite section) to the normal unit 36 (top of composite section), as listed in Table 2.

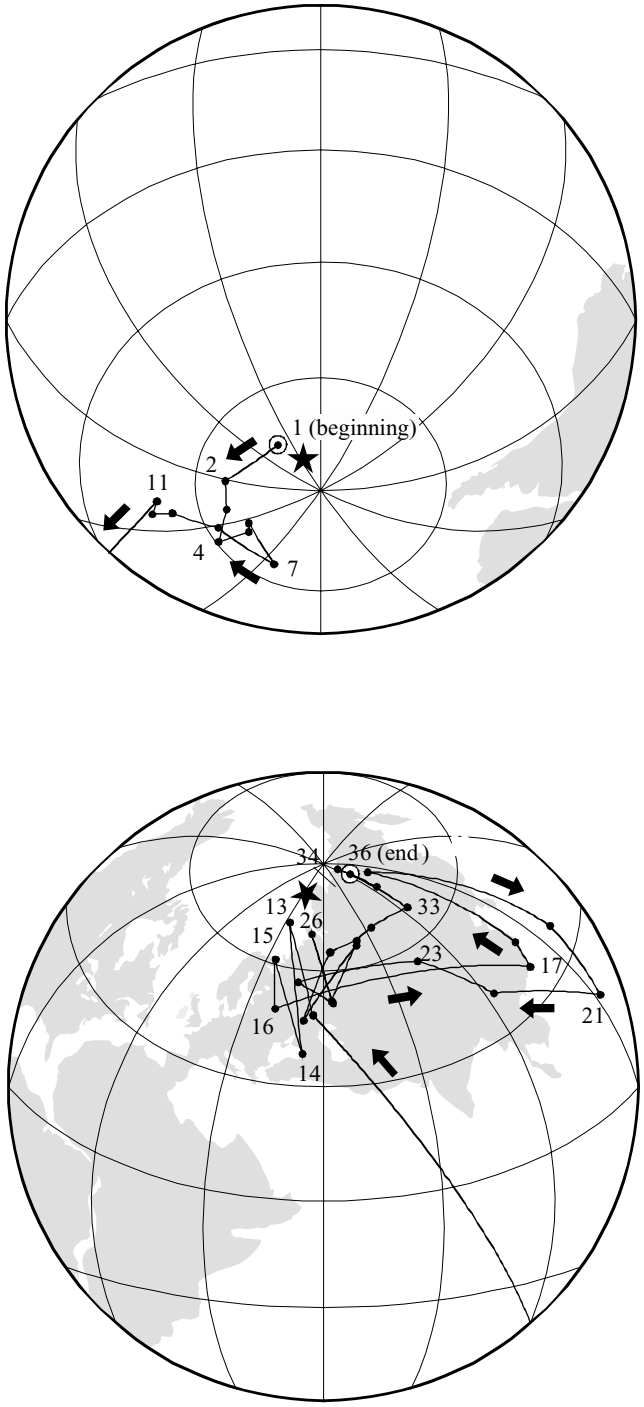

Figure 7. Equal-area projection of virtual palaeopole positions during the Lesotho reversal as recorded along the Bushmen's Pass composite section. Main continents (with present contours) and VGPs have been rotated according to the 180 Myr old plate reconstruction proposed by Morgan (1983). The palaeogeographic reference frame is pinned to the global palaeopole position for the period 175–200 Ma (Prévot *et al.* 2000). Star show the rotated position of the local palaeomagnetic pole obtained by Kosterov & Perrin (1996) from normal and reversed sequences from the Lesotho Basalt. Projection poles are (30°N, 60°E) for the northern hemisphere and (45°S, 240°E) for the southern hemisphere.

we used the remanence intensity after cleaning either by a 10 mT alternating field or heating at 200 °C. A decrease in remanence intensity is observed in the transition zone (Fig. 8), in qualitative agreement with the palaeointensity results of van Zijl *et al.* (1962b) who suggested a four- to fivefold diminution in field intensity. A more representative estimate of the specific magnetization decrease can be obtained by calculating the average magnetization intensity versus consecutive reversal angle intervals (Fig. 9). A rapid decrease is observed as soon as the reversal angle starts increasing. For reversal angles exceeding 20° the remanence intensity is reduced to approximately 15 per cent of the value found for the directions lying within a 10° radius cone from the average steady field direction.

5 DISCUSSION AND CONCLUSIONS

The present data confirm the suggestion of van Zijl *et al.* (1962b) that, due to a pause in volcanic activity that occurred apparently

Downloaded from https://academic.oup.com/gji/article/155/2/367/596587 by Univ of California, San Diego Library - INACTIVE user on 11 March 2025

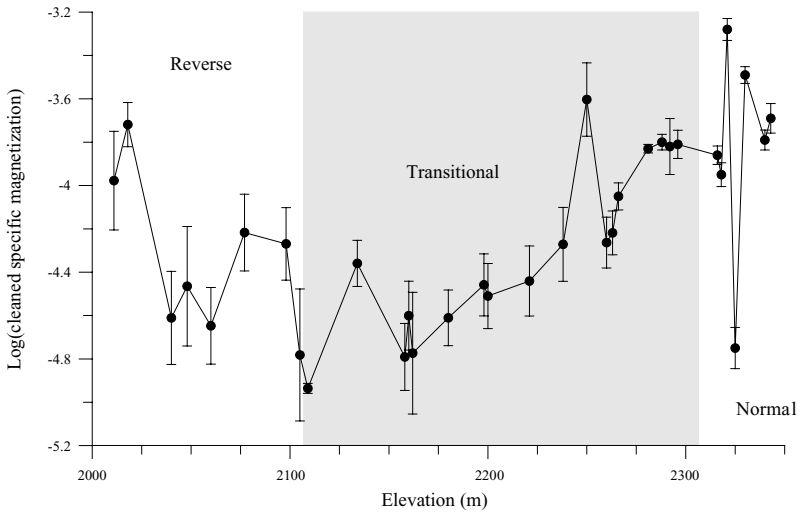

Figure 8. Cleaned specific magnetization (logarithmic scale) of palaeomagnetic units 1 to 36 (except 10) plotted in function of the elevation of the base of the unit.

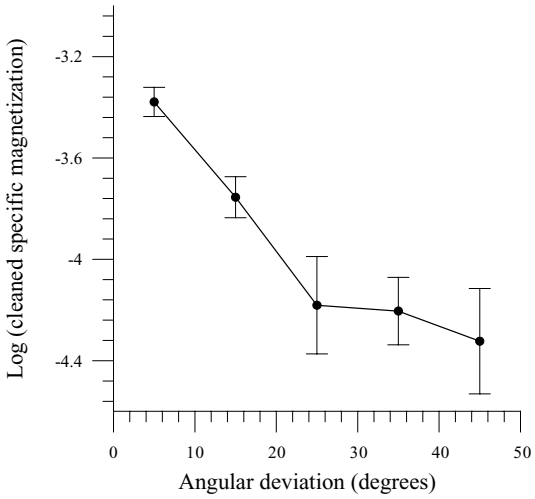

Figure 9. Cleaned specific magnetization (logarithmic scale) of palaeomagnetic units 1–36 (except 10) averaged over five adjacent 10° wide intervals of the reversal angle. By convention, the average magnetization is plotted at the middle of the corresponding interval of the reversal angle: 5°, 15°, 25°, 35° and 45°.

just during the most transitional stages, the Lesotho reversal is incompletely recorded. No VGP very close to the palaeoequator is observed. Considering that the global palaeopole is located at latitude 69.1° and longitude 311.4° for the period 175–200 Ma (Prévot *et al.* 2000), the lowest palaeolatitude of transitional VGP is 20° (unit 21, Fig. 7). The fluctuations of the transitional field directions documented by the present study are, however, quite different from those reported by van Zijl *et al.* (1962b). Also, they seem to have been rather gradual, with no compelling evidence in favour of the 'jerky' behaviour of the geomagnetic field advocated by those workers.

Both before and during the Lesotho reversal, several 'directional flow groups'—each constituted of consecutive flows exhibiting the same direction (within experimental uncertainties)—are found. Such directional flow groups are of rather common occurrence in volcanic sequences (e.g. Mankinen *et al.* 1985; Hoffman 1991; McElhinny *et al.* 1996; Széréméta *et al.* 1999). In the case of the Lesotho sequence, such groups comprise up to six consecutive flows (direction 2) but, more commonly, only three to five (directions 5, 11, 22 and 29). Directional groups can be interpreted either as multiple records of a single direction of a constantly changing geomagnetic field that are due to a brief outburst of volcanic activity (Mankinen *et al.* 1985) or as reflecting a standstill of the geomagnetic field direction (Hoffman 1991). The first interpretation is supported by many observations on present volcanoes. However, the second interpretation can be preferred when significant changes in field palaeostrength are observed within a single directional group (Prévot *et al.* 1985b) or, alternatively, when stratigraphically distinct directional flow groups recurrently record a similar field direction. Such a case can be observed in the detailed record of the reversal found at Steens Mountain (Mankinen *et al.* 1985; Camps *et al.* 1999) in which directional flow groups 21 (three consecutive flows) and 31 (seven consecutive flows) do yield the same transitional direction. Recently, a similar field recurrence was reported from another volcanic record of a mid-Miocene geomagnetic reversal found in Gran Canaria (Leonhardt *et al.* 2002). In contrast, the transitional directions carried by the flow groups from the Lesotho record are all different from each other. Given the absence of recurrent palaeomagnetic direction, we consider that these groups of flows are probably due to intense outpouring of several lava flows in a short interval of time rather than to successive standstills of the geomagnetic field.

Two successive N–I–N rebounds of the geomagnetic field towards intermediate VGPs are observed during the last stage of the Lesotho reversal after a first re-establishing of normal polarity (Fig. 7). Rebounds are commonly observed in detailed Cenozoic records of reversals (Mankinen *et al.* 1985; Chauvin *et al.* 1990; Kristjansson & Sigurgeirsson 1993; Leonhardt *et al.* 2002). Palaeomagnetic records of Cenozoic reversals obtained from sedimentary rocks indicate that transitional poles tend to fall along two longitude bands centred on America or Asia/Pacific boundary (Laj *et al.* 1991; Tric *et al.* 1991). The significance of this pattern is unclear. If not weighted, transitional poles from volcanic rocks from the past 16 Myr show no evidence for any longitudinal organization (Prévot & Camps 1993). However, using debatable methods of normalization and weighting, Love (1998) observed a maximum in the VGP longitude distribution between 60° and 90°E (Eastern Asia). Intriguingly, the rebound VGPs of the Lesotho reversal fall along the boundary between the Eurasia and Pacific plates. However, in the absence of other data from geomagnetic reversals with appropriate dates, we do not know whether this observation is representative for the Jurassic.

Downloaded from https://academic.oup.com/gji/article/155/2/367/596587 by Univ of California, San Diego Library - INACTIVE user on 11 March 2025

The regularity of the decrease in averaged specific magnetization as the transitional field deviates from the normal/reverse field direction (Fig. 9) strongly suggests that this diminution reflects a progressive decrease of the geomagnetic palaeostrength. Quite similar trends were reported from Cenozoic volcanic sequences in Iceland (Kristjansson 1985) and Polynesia (Chauvin *et al.* 1990). Such trends are well fitted by a statistical model of the geomagnetic field in which the fluctuations of the non-axial dipole components are isotropic and independent from those of the axial dipole (Camps & Prévot 1996). The trend in magnetization magnitude versus reversal angle (Fig. 9) suggests that the maximum decrease in the palaeofield intensity might have reached 80–90 per cent during the Lesotho reversal, which is comparable with the result obtained from direct palaeointensity measurements for the well-documented Cenozoic Steens Mountain reversal (Prévot *et al.* 1985b). Taking into account the weakness of the local steady palaeofied in the Early Jurassic (24 ± 11 μT according to Kosterov & Perrin 1996), the predicted transitional field intensity would have been particularly low. The variation of the averaged specific magnetization as the field reverses (Fig. 8) suggests some asymmetry in the change in field magnitude from the pre- to the post-transitional stages. A similar behaviour is well substantiated by direct palaeostrength determinations on several Cenozoic geomagnetic reversals (Prévot *et al.* 1985b; Bogue & Paul 1993; Riisager & Abrahamsen 2000).

Thus, although the palaeomagnetic data for the Lesotho reversal are not as complete and accurate as for more recent reversals, they support the contention that the characteristics of geomagnetic reversals were similar in Late Cenozoic and Early Jurassic times. While the long-term averaged dipole moment of the Earth appears to have been half the strength during the Early Jurassic compared with the Late Cenozoic (Prévot *et al.* 1990; Kosterov *et al.* 1997; Perrin & Shcherbakov 1997), the reversal process seems to have been basically unchanged.

ACKNOWLEDGMENTS

We are indebted to the Institute of Southern African Studies, Lesotho and its Director, Prof. K. K. Prah, for welcoming three of us (MP, NR and JT) as Visiting Research Associates at the National University of Lesotho in 1986 and to J. S. van Zijl who then kindly joined us in the field during the Bushmen's Pass section. The paper benefited from reviewer comments from C. Laj, A. Mazaud, and an anonymous reviewer. The work was supported by CNRS-INSU (programmes 'ATP Noyau 1986' and 'Terre Profonde 1991') and a personal fellowship to NR from the NERC.

REFERENCES

Bogue, S.W. & Paul, H.A., 1993. Distinctive field behavior following geomagnetic reversals, *Geophys. Res. Lett.,* **20,** 2399–2409.

Brynjolfsson, A., 1957. Studies of remanent magnetism and viscous magnetism in the basalts of Iceland, *Phil. Mag. Sup.,* **6,** 247–254.

Camps, P. & Prévot, M., 1996. A statistical model of the fluctuations in the geomagnetic field from palaeosecular variation to reversal, *Science,* **273,** 776–779.

Camps, P., Coe, R.S. & Prévot, M., 1999. Transitional geomagnetic impulse hypothesis: geomagnetic fact or rock-magnetic artifact?, *J. geophys. Res.,* **104,** 17 747–17 758.

Chauvin, A., Roperch, P. & Duncan, R.A., 1990. Records of geomagnetic reversals from volcanic islands of French Polynesia 2. Palaeomagnetic study of a flow sequence (1.2–0.6 Ma) from the island of Tahiti and discussion of reversal models, *J. geophys. Res.,* **95,** 2727–2752.

Cox, K.G., 1988. The Karoo province, in *Continental Flood Basalts,* pp. 239–271, ed. MacDougall, J.D.

Dagley, P. & Wilson, R.L., 1971. Geomagnetic field reversals—a link between strength and orientation of a dipole source, *Nature Phys. Sci.,* **232,** 16–18.

Duncan, R.A., Hooper, P.R., Rehacek, J., Marsh, J.S. & Duncan, A.R., 1997. The timing and duration of the Karoo igneous event, southern Gondwana, *J. geophys. Res.,* **102,** 18 127–18 138.

Fitch, F.J. & Miller, J.A., 1971. Potassium–argon radioages of Karoo volcanic rocks, *Bull. volcan.,* **35,** 64–84.

Fitch, F.J. & Miller, J.A., 1984. Dating Karoo igneous rocks by the conventional K-Ar and $^{40}Ar/^{39}Ar$ age spectrum methods, *Spec. Publ. geol. Soc. S. Afr.,* **13,** 247–266.

Goguitchaichvili, A.T., Prévot, M. & Camps, P., 1999. No evidence for strong fields during the R3–N3 Icelandic geomagnetic reversal, *Earth planet. Sci. Lett.,* **167,** 15–34.

Gradstein, F.M., Frits, P.A., Ogg, J.G., Hardenbol, J., van Veen, P., Thierry, J. & Huang, Z., 1994. A Mesozoic time scale, *J. geophys. Res.,* **99,** 24 051–24 074.

Hargraves, R.B., Rehacek, J. & Hooper, P.R., 1997. Palaeomagnetism of the Karoo igneous rocks in southern Africa, *South African J. Geol.,* **100,** 195–212.

Hoffman, K.A., 1991. Long-lived transitional states of the geomagnetic field and the two dynamo families, *Nature,* **354,** 273–277.

Kirschvink, J.L., 1980. The least-squares line and plane and the analysis of palaeomagnetic data, *Geophys. J. R. astr. Soc.,* **62,** 699–718.

Kosterov, A.A. & Perrin, M., 1996. Palaeomagnetism of the Lesotho Basalt, Southern Africa, *Earth planet. Sci. Lett.,* **139,** 63–78.

Kosterov, A.A. & Prévot, M., 1998. Possible Mechanism causing failure of the Thellier palaeointensity experiments in some basalts, *Geophys. J. Int.,* **134,** 554–572.

Kosterov, A.A., Prévot, M., Perrin, M. & Shashkanov, V.A., 1997. Palaeointensity of the Earth's magnetic field in Jurassic: new results from a Thellier study of the Lesotho basalt, Southern Africa, *J. geophys. Res.,* **102,** 24 859–24 872.

Kristjansson, L., 1985. Some statistical properties of palaeomagnetic directions in Icelandic lava flows, *Geophys. J. R. astr. Soc.,* **80,** 57–71.

Kristjansson, L. & Sigurgeirsson, M., 1993. The R3–W3 and R5–N5 paleomagnetic transition zones is SW-Iceland Revisited, *J. geomag. geoelectr.,* **45,** 275–288.

Laj, C., Mazaud, A., Weeks, R., Fuller, M. & Herrero-Bervera, E., 1991. Geomagnetic reversal paths, *Nature,* **351,** 447.

Leonhardt, R., Matzka, J., Hufenbecher, F. & Soffel, H.C., 2002. A reversal of the Earth's magnetic field recorded in mid-Miocene lava flows from Gran Canaria: palaeodirections, *J. geophys. Res.,* **107,** 10.1029/2001JB000322.

Love, J.J., 1998. Palaeomagnetic volcanic data and geometric regularity of reversals and excursions, *J. geophys. Res.,* **103,** 12 435–12 452.

McElhinny, M.W., McFadden, P.L. & Merrill, R.T., 1996. The myth of the Pacific dipole window, *Earth planet. Sci. Lett.,* **143,** 13–22.

Mankinen, E.A., Prévot, M., Grommé, C.S. & Coe, R.S., 1985. The Steens Mountain (Oregon) geomagnetic polarity transition 1. Directional history, duration of episodes, and rock magnetism, *J. geophys. Res.,* **90,** 10 393–10 416.

Morgan, W.J., 1983. Hotspot tracks and the early rifting of the Atlantic, *Tectonophysics,* **94,** 123–139.

Néel, L., 1951. L'inversion de l'aimantation permanente des roches, *Ann. Géophys,* **7,** 90–102.

Néel, L., 1952. Confirmation expérimentale d'un mécanisme d'inversion de l'aimantation thermorémanente, *C.R. Acad. Sci.,* **234,** 1991–1993.

Perrin, M. & Shcherbakov, V., 1997. Palaeointensity of the Earth's magnetic field for the past 400 Ma: evidence for a dipole structure during the Mesozoic low, *J. Geomag. Geoelect.,* **49,** 601–614.

Prévot, M., 1981. Some aspects of magnetic viscosity in subaerial and submarine volcanic rocks, *Geophys. J. R. astr. Soc.,* **66,** 169–192.

Prévot, M. & Camps, P., 1993. Absence of preferred longitude sectors for poles from volcanic records of geomagnetic reversals, *Nature,* **366,** 53–57.

Downloaded from https://academic.oup.com/gji/article/155/2/367/596587 by Univ of California, San Diego Library - INACTIVE user on 11 March 2025

Prévot, M., Mankinen, E.A., Grommé, C.S. & Coe, R.S., 1985a. How the geomagnetic field vector reverses polarity, *Nature,* **316,** 230–234.

Prévot, M., Mankinen, E.A., Coe, R.S. & Grommé, C.S., 1985b. The Steens Mountain (Oregon) geomagnetic polarity transition 2. Field intensity variations and discussion of reversal models, *J. geophys. Res.,* **90,** 10 417–10 448.

Prévot, M., Derder, M.M., McWilliams, M. & Thompson, J., 1990. Intensity of the Earth's magnetic field: evidence for a Mesozoic dipole low, *Earth planet. Sci. Lett.,* **97,** 129–139.

Prévot, M., Mattern, E., Camps, P. & Daignières, M., 2000. Evidence for a 20° tilting of the Earth's rotation axis 110 million years ago, *Earth planet. Sci. Lett.,* **179,** 517–528.

Riisager, P. & Abrahamsen, N., 2000. Palaeointensity of West Greenland Palaeocene basalts: asymmetric intensity around the C27n–C26r transition, *Phys. Earth planet. Inter.,* **118,** 53–64.

Sigurgeirsson, T., 1957. Direction of magnetization in Icelandic basalts, *Phil. Mag. Sup.,* **6,** 240–246.

Széréméta, N., Laj, C., Guillou, H., Kissel, C., Mazaud, A. & Carracedo, J.-C., 1999. Geomagnetic palaeosecular variation in the Brunhes period, from the island of El Hierro (Canary Island), *Earth planet. Sci. Lett.,* **165,** 241–253.

Thellier, E. & Thellier, O., 1944. Recherches géomagnétiques sur les coulées volcaniques d'Auvergne, *Ann. Géophys.,* **1,** 37–52.

Thellier, E. & Thellier, O., 1959. Sur l'intensité du champ magnétique terrestre dans le passé historique et géologique, *Ann. Géophys.,* **15,** 285–376.

Tric, E., Laj, C., Jéhanno, C., Valet, J.P., Mazaud, A., Kissel, C. & Iaccarino, S., 1991. High-resolution record of the Upper Olduwai transition from Po valley (Italy) sediments: support for dipolar transition geometry?, *Phys. Earth planet. Inter.,* **65,** 319–336.

van Zijl, J.S.V., Graham, K.W.T. & Hales, A.L., 1962a. The palaeomagnetism of the Stormberg lavas of South Africa 1: evidence for a genuine reversal of the Earth's field in Triassic–Jurassic times, *Geophys. J. R. astr. Soc.,* **7,** 23–39.

van Zijl, J.S.V., Graham, K.W.T. & Hales, A.L., 1962b. The palaeomagnetism of the Stormberg lavas of South Africa 2: the behaviour of the magnetic field during a reversal, *Geophys. J. R. astr. Soc.,* **7,** 169–182.

Watkins, N.D., 1969. Non-dipole behaviour during an Upper Miocene geomagnetic polarity transition in Oregon, *Geophys. J. R. astr. Soc.,* **17,** 121–149.

Downloaded from https://academic.oup.com/gji/article/155/2/367/596587 by Univ of California, San Diego Library - INACTIVE user on 11 March 2025